NAVWEPS REPORT 8071
NOTS TP 3086
COPY 68

AN ANGULAR TRACKING DRIVE FOR A RADIO TELESCOPE OF UNCONVENTIONAL DESIGN

By

John M. Boyle
Aviation Ordnance Department

ABSTRACT. This report describes the reflector support and drive system for a large radio telescope of unconventional design. The telescope consists of a hollow sphere supported in a hydrostatic bearing formed by a concave socket filled with water. A simple system of water pressure pads driven by a positive displacement pump keeps the sphere centered in the socket.

The drive system consists of a pulsed air jet or rocket motor that rotates about the axis of the telescope directly in front of the feed antenna. The drive system is unique in that it is independent of the orientation of the telescope with respect to the earth.

The theoretical and experimental portions of this report analyze the performance of the drive system of a two-foot-diameter model which automatically tracks an X-band source.

U.S. NAVAL ORDNANCE TEST STATION

China Lake, California

December 1962

U. S. NAVAL ORDNANCE TEST STATION

AN ACTIVITY OF THE BUREAU OF NAVAL WEAPONS

C. BLENMAN, JR., CAPT., USN
Commander

WM. B. McLEAN, PH.D.
Technical Director

FOREWORD

This study has been made to determine the feasibility of a large radio telescope to be used for astronomical studies or for space communications.

Preliminary investigations have shown that the Naval Ordnance Test Station would be a suitable location for a telescope of modest size and cost, of the type described in this report. It is hoped such a telescope may be constructed here in the future.

This work has been done under WEPTASK R360-FR 112/216-1/F008-01-24, and this report has been reviewed for technical accuracy by James W. Oestreich and Arnold A. Moline.

Released by
N. E. WARD, Head
Aviation Ordnance Department
10 October 1962

Under authority of
WM. B. McLEAN
Technical Director

NOTS Technical Publication 3086
NAVWEPS Report 8071

Published by.....Aviation Ordnance Department
Manuscript.....35/MS-173
Collation.....Cover, 16 leaves, abstract cards
First printing.....170 numbered copies
Security classification.....UNCLASSIFIED

CONTENTS

Figures:

ACKNOWLEDGMENT

The author wishes to thank Mr. James Oestreich of the Naval Ordnance Test Station for his guidance in the operation of the analog computing facilities.

INTRODUCTION

This report discusses construction and drive problems encountered in large radio telescopes. The conventionally designed radio telescope is first discussed briefly; a proposed telescope of unconventional design is discussed more fully.

In a large radio telescope of conventional design that consists of a circular parabolic reflector mounted on an equatorial or an altazimuth mount, the principal problems encountered are:

1. Insufficient rigidity in the structure supporting the reflector,

2. Excessive stress concentrations in the telescope drive mechanism due to the enormous weight in the movable structure, and

3. Inadequate servo drive performance due to the geometric limitations of the simple altazimuth mounts dictated in the design of conventional large telescopes.

Two of the main demands placed on radio telescopes are gain and directivity. These demands are satisfied by aperture. A third demand is for broad frequency capability. The parabola of revolution represents the most compact shape that will satisfy these requirements, particularly if the telescope is made steerable.

The drive mechanisms for steerable paraboloids have fallen into two classes: equatorial and altazimuth. Considerable research has shown that the altazimuth mount is the more feasible for reflectors with diameters larger than 150 feet.[1]

The altazimuth mount is not particularly desirable for astronomy because the normal hour angle and declination coordinates must be converted to elevation and azimuth. In addition, sources near zenith are difficult to track because of the large azimuth rates involved.

As the diameter of the telescope is increased to hundreds of feet, additional problems are encountered that are concerned with making the paraboloid retain its contour with variations in pointing angle and wind loading. The design of the 600-foot-diameter radio telescope now under construction at Green Bank, West Virginia, is an attempt to obtain the

[1] Emberson, R. M., and N. L. Ashton. "The Telescope Program for the National Radio Astronomy Observatory at Green Bank, West Virginia," PROC IRE, January 1958, pp. 23-35.

maximum stiffness in the antenna-supporting structure.[2] An artist's conception of the completed structure is shown in Fig. 1.. The structure behind the reflector is a cylindrical network of girders that support both the reflecting surface and the elevation drive. The support rollers for the cylinder are attached to a carriage that in turn is supported by trucks riding on a circular track to afford azimuth rotation. The stress concentration at many points in the structure could be severe; the weight of the movable structure will be approximately 21,000 tons.

A 600-foot-diameter aperture is not the ultimate in size; several studies show a need for antennas greater than 1,000 feet in diameter.[3] A 1,000-foot-diameter fixed reflector with steerable feed is being constructed in Puerto Rico. Here, sky coverage is restricted to plus or minus 20 degrees of the zenith.[4]

The proposed radio telescope described in this report consists of a hollow sphere supported in a hydrostatic bearing formed by a concave socket filled with water. A simple system of water pressure pads driven by positive displacement pumps keeps the sphere centered in the socket.

The drive system consists of a pulsed air jet or rocket motor that rotates about the axis of the telescope directly in front of the feed antenna. The system is unique in that it is independent of the orientation of the telescope with respect to the earth.

The reflector support and drive for the proposed telescope is described in the next section. The design should overcome, at least in part, the problems that have been previously mentioned. The advantages claimed for the configuration are:

1. The angular restrictions of the equatorial and altazimuth drives are avoided, since the telescope tracking system is divorced from earth coordinates.

2. The strongest possible shape has been chosen for the supporting structure, i.e., a sphere.

3. The weight of the reflector and its spherical support are borne by a very large area so that stress concentration with its attendant structural distortion is minimized.

---

[2] McClain, Edward F., Jr., "The 600-Foot Radio Telescope," Scientific American, Vol. 202, January 1960, pp. 45-51.

[3] Heeschen, D. S., and N. H. Dieter. "Extragalactic 21-cm Line Studies," PROC IRE, Vol. 46, January 1958, pp. 23-35.

[4] Gordon, W. E., and L. M. LaLonde. "The Design and Capabilities of An Ionospheric Radar Probe," PROC IRE, Transactions or Antennas and Propagation, Vol. AP-9, January 1961.

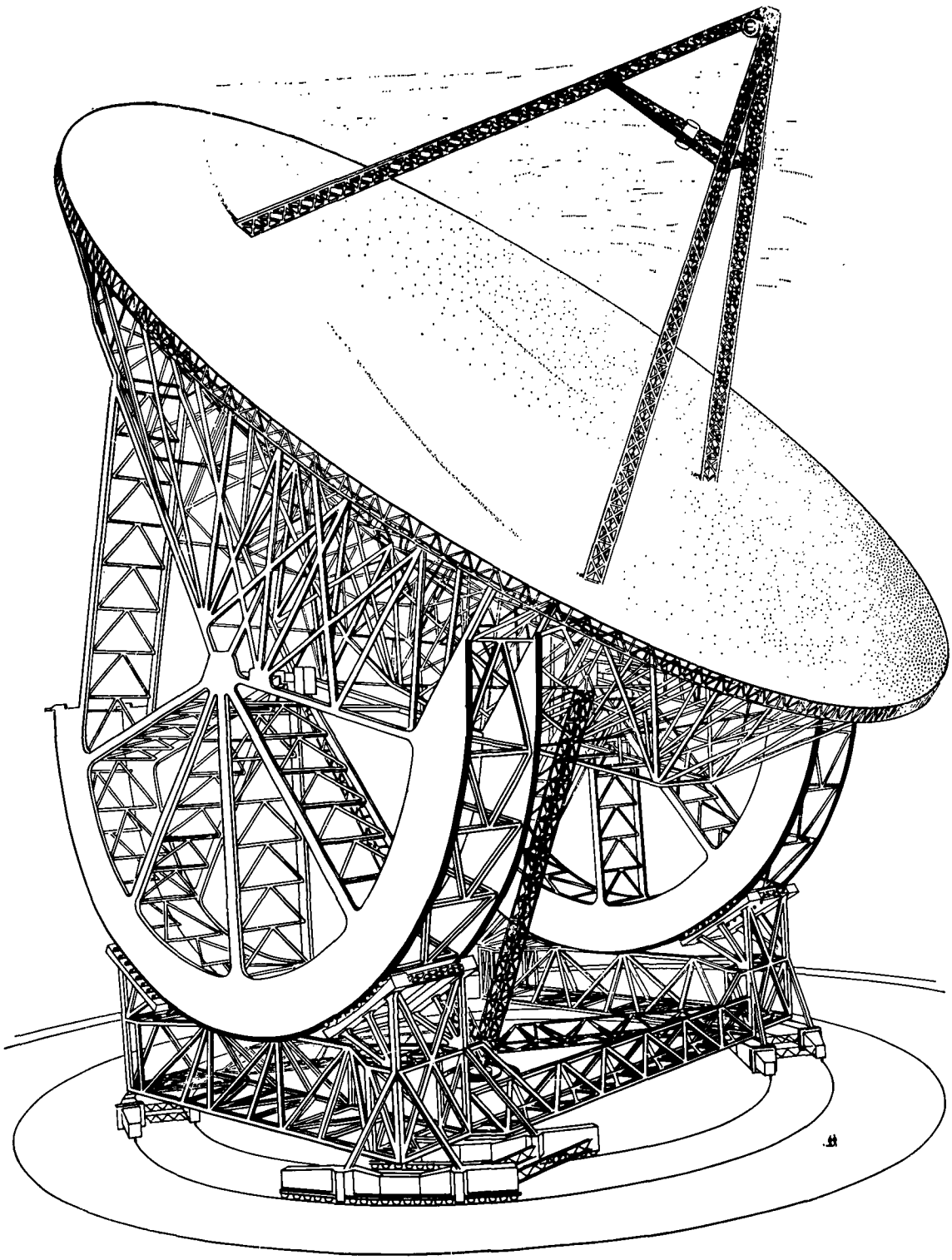

FIG. 1. Artist's Conception of 600-Foot-Diameter Radio Telescope. (Reprinted by permission of the Scientific American.)

The parameters of a two-foot-diameter model of the telescope have been measured and analyzed on an analog computer. The results of the computer investigation not only agreed with the performance of the model, but indicated the changes that should be made in system parameters to attain an optimum servo design.

CONSTRUCTION OF THE TELESCOPE MODEL

The circular parabolic reflector is embedded in the sphere in such a way that its edge lies on the sphere's surface; the diameter of the reflector is approximately 0.8 of the diameter of the sphere.

The sphere floats in water contained in a concave socket atop the support pedestal and is centered in the socket by the action of the pressure pads that are arranged every 120 degrees about the periphery of the socket. Each pressure pad is supplied with water by a constant displacement pump that recirculates the overflow water from the socket. If the sphere starts to drift horizontally from its center position, the flow of water out of the pressure pad is restricted on the side of the socket toward which the sphere is drifting. As the flow of the pump supplying the pad is restricted, the water pressure increases in order to maintain the flow rate constant. This increased pressure results in an increased force being exerted on the sphere by the pressure pad which opposes lateral movement of the sphere. An equilibrium point is reached at which the horizontal force exerted on the sphere by wind loads is balanced by the force of the pressure pad. In most cases the wind loads are borne by two adjacent pressure pads, each supplying the necessary component of the opposing force.

There are three main types of angular-position commands which a radio telescope should be able to accept:

1. To point along a certain line relative to the earth,
2. To point along a certain line relative to inertial space, and
3. To track some object automatically while the object is radiating or reflecting electromagnetic energy.

The theoretical and experimental portions of this report analyze a system set up to deal with the third type of position commands. The turning torque is supplied by a pulsed air jet which rotates in synchronism with the conically scanning feed antenna located at the focus. Tests with the two-foot-diameter model confirmed the soundness of the design and pointed up any difficulties which might be encountered in a full-sized unit. Figure 2 is a photograph of the completed model, and Fig. 3 is a close-up photograph of the mechanism located at the focus.

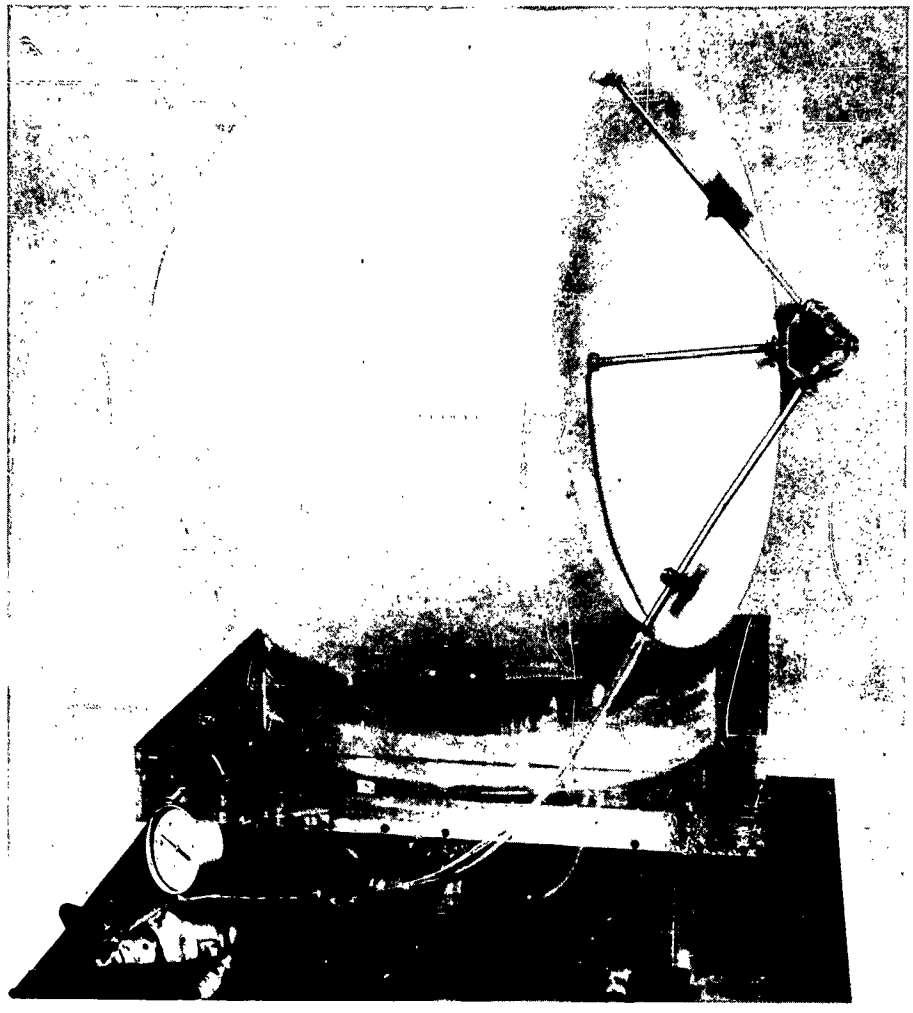

FIG. 2. Two-Foot-Diameter Model of Radio Telescope.

The two-foot-diameter sphere was machined from a solid block of foamed polystyrene having a density of approximately two pounds per cubic foot and then coated with epoxy resin. The resin was in turn machined to form a thin shell with a thickness of approximately 0.050 inch. The thin shell, backed by low-density foam, forms an extremely rigid structure.

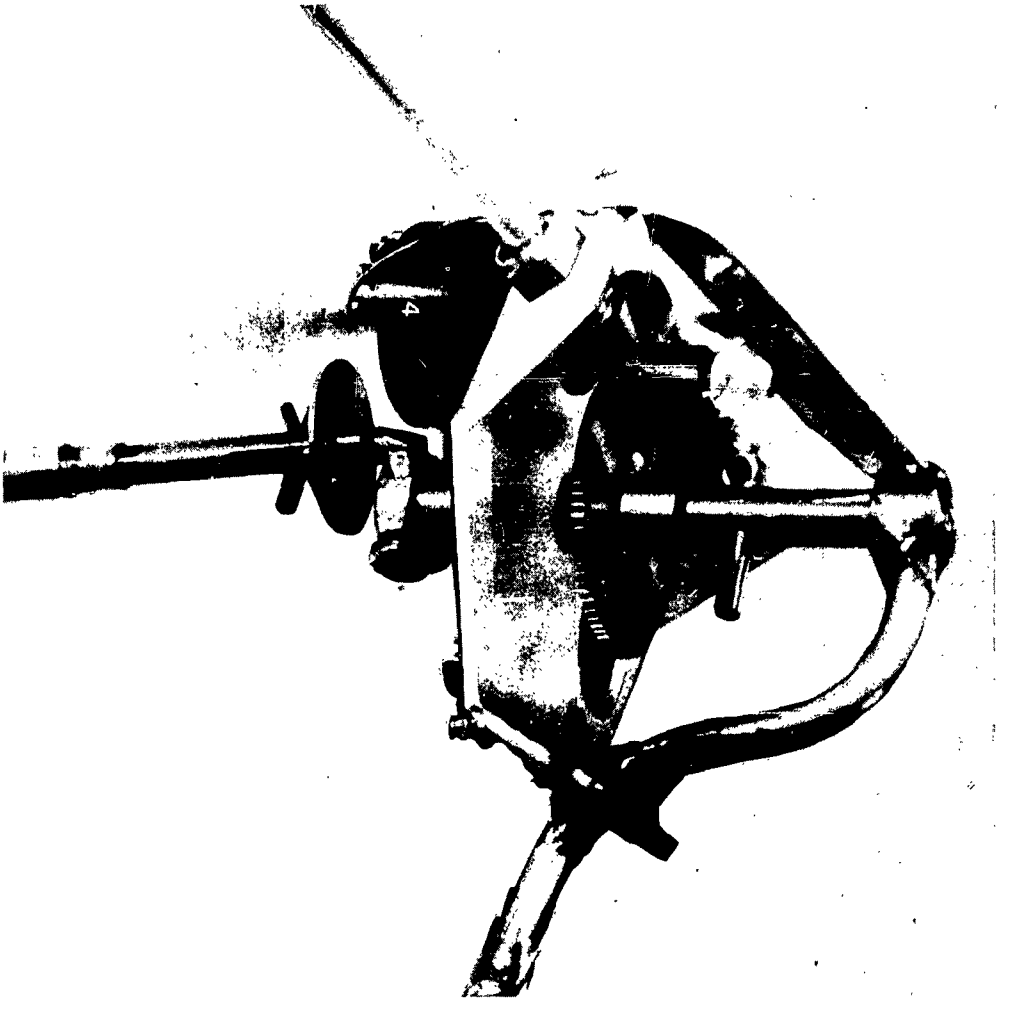

FIG. 3. Mechanism Located at Focus.

The reflecting surface was first roughed out of the polystyrene foam on a lathe and then placed on a precision rate-of-turntable so that the axis of the desired reflector was vertical. A reflector was centrifugally cast by rotating the turntable at the proper speed to generate a paraboloid of the desired focal length (see Appendix A). Epoxy resin was used as the casting agent and the surface was coated with conductive silver paint to complete the reflector.

A tubular aluminum tripod supports the scanner mechanism, feed antenna, and the air jet in front of the reflector. The scanner mechanism consists of a 3-watt, 400-cycle servo motor driving a speed-reduction gear train to produce a 3-revolution-per-second (rps) speed on the scanner

shaft that lies on the axis of the parabolic reflector. The inner end of the scanner shaft passes through a bearing and is fastened to a crank in order to impart a nutating motion to the feed antenna, a crossed-dipole ground-plane variety that is designed to operate at 9,400 megacycles (mc). The crank throw is about 0.230 inch in order to offset the axis of the antenna beam by about one half the beam width, or 2 degrees. A silicon microwave crystal video detector, Sylvania Type IN 358A, is connected to the coaxial line of the feed antenna. The crystal output is proportional to the 9,400-mc input to the antenna. This output is conveyed by shielded flexible cable through the antenna support post to the vertex of the reflector, and thence to the edge of the reflector, where it is bundled with the scanner motor leads and the flexible air hose. The antenna support post serves to hold the feed antenna-detector assembly in alignment with the reflector and to prevent it from turning. Flexibility of mounting of the inner end of the post is provided by an O-ring located in a socket at the reflector vertex.

The outer end of the scanner shaft is hollow and terminates in a bearing which supports the shaft and acts as a rotating joint to convey the compressed air used to drive the telescope. Air exhausts from the scanner shaft through a nozzle perpendicular to it.

The moving portion of the telescope must be carefully balanced to eliminate any residual torques in any position. It was convenient to accomplish this by means of small polyethylene tubes filled with lead shot and attached to the feed support tripod at appropriate places.

OPERATION OF THE TELESCOPE MODEL

GENERAL PRINCIPLES

The feed antenna is driven in a circle about the focal point of the paraboloid by the scanner mechanism at a frequency ω_s. If the reflector is pointed at a distant source, the energy intercepted by the telescope is reflected to the focus. The radius of the circle described by the feed antenna is chosen so that the power intercepted by the feed antenna is approximately 3 decibels (db) below what it would be if the feed antenna were located at the focus. The signal received by the feed antenna does not vary as long as the focus of the energy remains centered in the circle.

If the source moves in angle with respect to the axis of the telescope, a pointing error angle, ϵ, is developed. As a result, the energy received by the telescope is no longer reflected to the focal point of the paraboloid but is displaced to one side by ϵ, if the approximations of simple geometric optics are allowed. Consequently, the signal received by the

feed antenna will no longer be constant, but will be sinusoidally modulated at the frequency ω_s. The modulation factor, $f(\epsilon)$, is a function of ϵ as shown in Fig. 4.[8] An additional property of this modulation is that its phase angle, α, relative to the phase of the scanner, indicates the position of the source relative to the axis of the telescope. These two pieces of information, amplitude and phase, contained by the modulation therefore locate in polar coordinates the position of the source relative to the axis of the telescope.

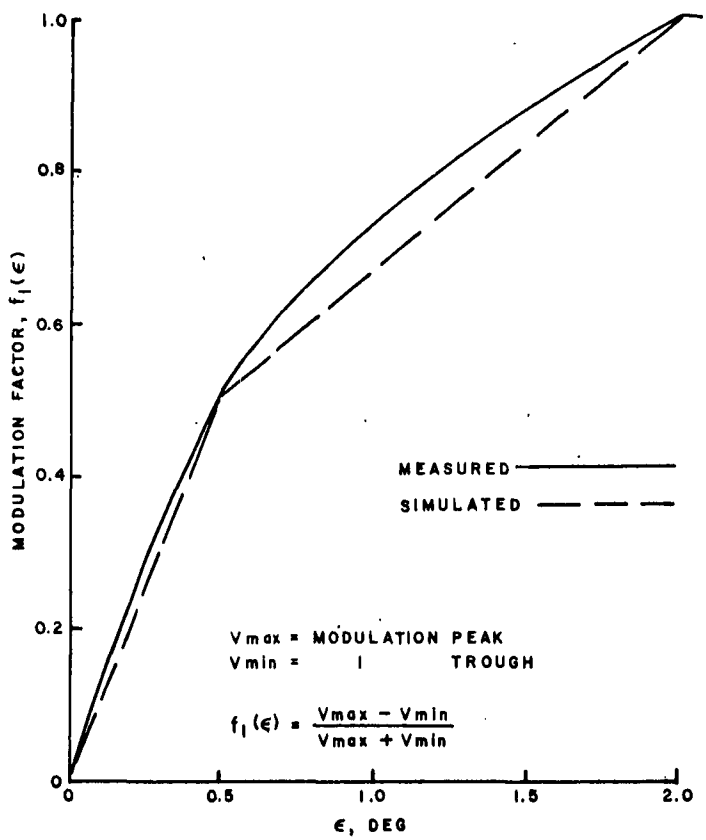

FIG. 4. Modulation Factor of the Scanner.

The expression for the detected output signal from the scanner can therefore be written

$$V_S = V_C \left[1 + f_1(\epsilon)\epsilon \sin (\omega_s t + \alpha)\right] , \qquad (1)$$

where

V_S = output voltage from IN358A detector (operating in linear region)

V_C = output voltage from IN358A if no pointing error is present

$f_1(\epsilon)$ = modulation factor of the scanner (see Fig. 4)

ϵ = pointing error angle

ω_s = scan frequency, about 18.8 radians per second (rad/sec)

α = position of source relative to the axis of the telescope.

The signal source used in the experiments conducted on the model was a 100-milliwatt (mw) reflex klystron operating at 9,400 mc and feeding a linearly polarized horn antenna with about + 17 db gain relative to an isotropic radiator. A 1,000-cycle square-wave modulation was imposed on the klystron reflector, resulting in 100% modulation of the klystron output.

Use of a 1,000-cycle modulated source allowed the amplifier stage Q_1 and Q_2 in the receiver to be AC coupled as shown in Fig. 5. Q_1 and Q_2 comprise a conventional feedback pair amplifier with a voltage gain of 500 to the secondary of T_1. When the telescope was pointed at the source, the 1,000-cycle modulated signal appearing across one half of the secondary of T_1 was 8 volts peak.

Germanium diodes D_1 and D_2, combined with the center-tapped secondary of T_1, form a full-wave rectifier circuit. D_1 and D_2 also perform the function of voltage comparators to derive the current pulses fed to the solenoid valve.

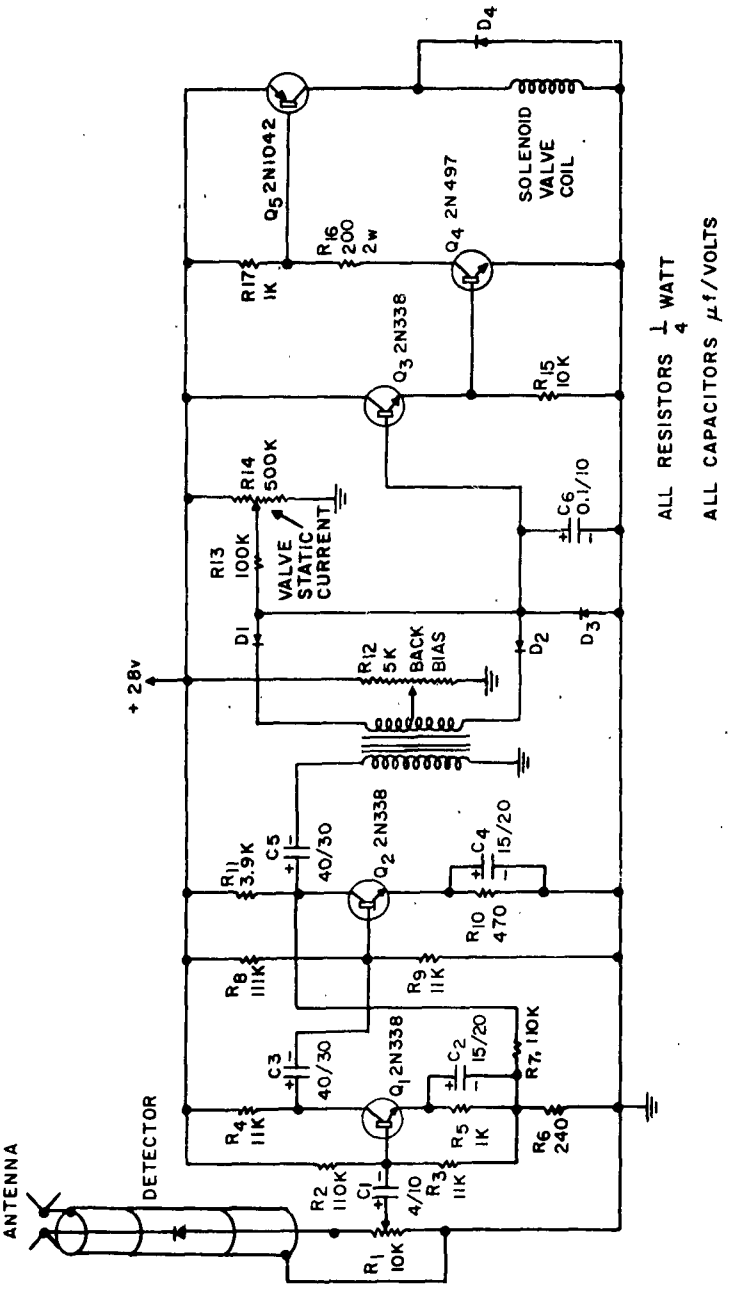

FIG. 5. Schematic of Amplifier.

Q_3, Q_4, and Q_5 make up a very high gain DC amplifier. The current gain of this combination is in the vicinity of 100,000. The valve static current control, R_{14}, is adjusted so that approximately +10 microamperes (μa) current is fed to the base of Q_3 in the absence of any signal. The resultant 1-ampere collector current in Q_5 opens the solenoid valve. The solenoid valve can be closed if more than -10 μa current is fed to the base of Q_3 from the voltage comparator circuit. D_3 prevents damaging the base-emitter junction Q_3 by excessive negative voltage from the voltage comparator.

The voltage comparator action of D_1 and D_2 is illustrated in Fig. 6.

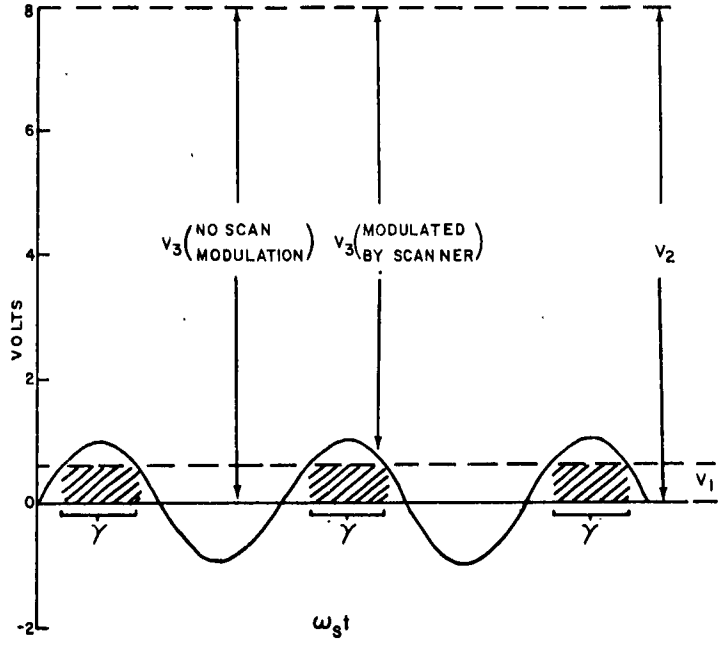

FIG. 6. Voltage Comparator Action.

V_1 is the voltage to ground at the base of Q_3 when no signal is present and Q_3 and Q_4 are conducting. V_1 is made up of the base to emitter junction drops of Q_3 and Q_4 in series. V_2 is the back bias applied to D_1 and D_2 by the setting of R_{12}.

When a signal is received from the source and no pointing error is present, a 1,000-cycle square wave of 8 volts peak amplitude appears across each half of the secondary of T_1. This voltage, V_3, will exceed the back bias V_2 and make diodes D_1 and D_2 conduct. Diode D_1 and D_2 conduct on alternate half cycles of the 1,000-cycle modulation. When D_1 and D_2 conduct, sufficient current flows to oppose the initial +10 μa base current flowing into Q_3, and the solenoid valve is de-energized, cutting off airflow. As long as no scan modulation corresponding to the telescope pointing error is present, the valve remains off.

When a pointing error, ϵ, appears, V_3 begins to be modulated since

$$V_3 = V_S(A) \quad , \tag{2}$$

where

A = voltage gain of amplifier from input of Q_1 to one half of the secondary of T_1.

If ϵ increases to the point that $V_2 - V_3$ exceeds V_1 during the negative scan modulation peaks, the diodes D_1 and D_2 will cease conducting and Q_3 will conduct, opening the solenoid valve. The flow of air through the valve will continue only as long as $V_2 - V_3$ is greater than V_1. It can be said that

$$\cos \frac{\gamma}{2} = \frac{V_1}{V_2 - V_3\ 1 - f_1(\epsilon)\epsilon} \tag{3}$$

or

$$\gamma = 2 \cos^{-1} \frac{V_1}{V_2 - V_3\ 1 - f_1(\epsilon)\epsilon} \quad .$$

The duration, γ, of the angular sector in which the valve is open is plotted in Fig. 7.

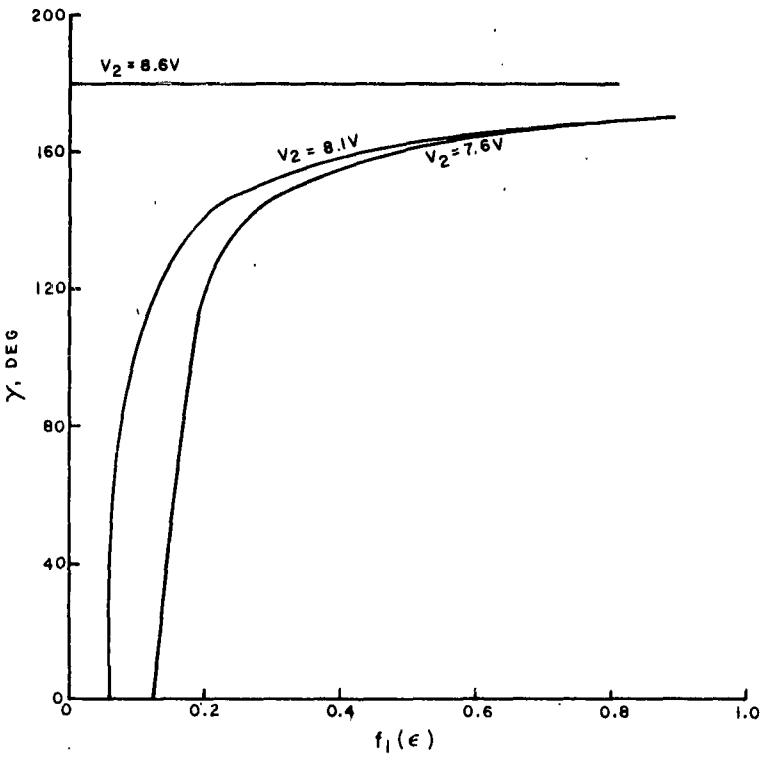

FIG. 7. Valve Open Time, γ, Versus Modulation Factor $f_1(\epsilon)$.

Another factor must be considered in determining the effective torque applied by the air jet to the telescope. The jet can be considered to be a rotating vector which can have a magnitude of either zero or a certain value at any instant, depending on whether it is off or on. By varying the width and timing of the air impulses, it is possible to drive the telescope in the direction necessary to follow the source. The normalized torque impulse per revolution, Z, is equal to $\sin \frac{\gamma}{2}$. When γ is small, the efficiency of the air jet is high. As γ approaches 180 degrees, the forces produced at the beginning and end of the air pulse tend to cancel each other. The variation of Z with γ is plotted in Fig. 8.

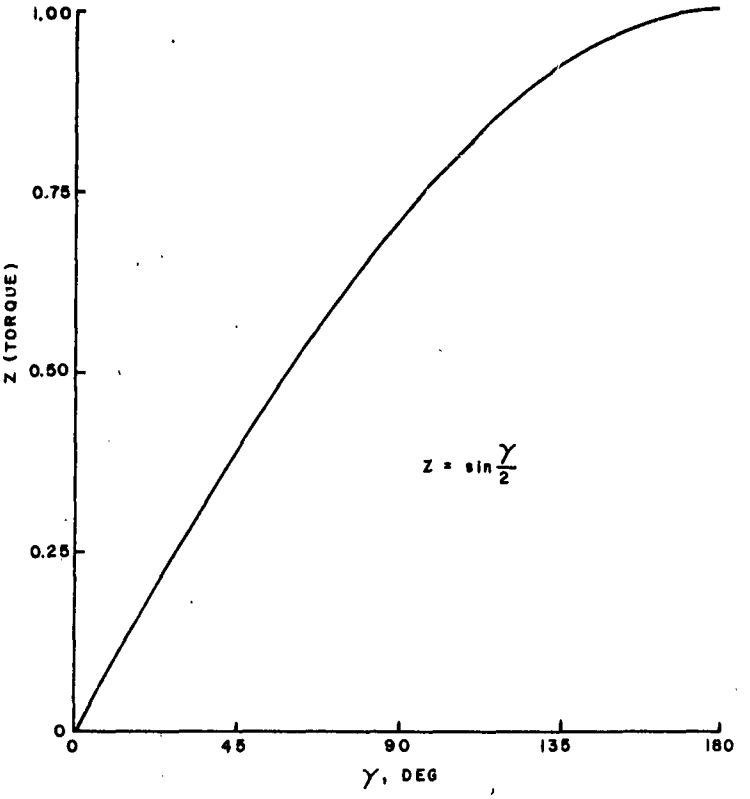

FIG. 8. Normalized Torque Impulse per Scanner Revolution, Z, Versus Valve Open Time, γ.

Proper adjustment of the phasing between the conical scanner and the air jet is accomplished by loosening set screws holding the antenna drive crank to the scanner shaft, rotating the crank to the desired phase angle, and then retightening the set screws. This phase adjustment will compensate for any fixed delays in the pulsing system. The main delay encountered is the opening and closing time of the solenoid valve, which is approximately 0.01 second, or about 10 degrees of rotation of the scanner shaft.

The next parameter in the telescope drive which must be considered is the thrust produced by the air jet. Figure 9 is the static thrust, F, of the air jet versus air pressure supplied at the solenoid valve.

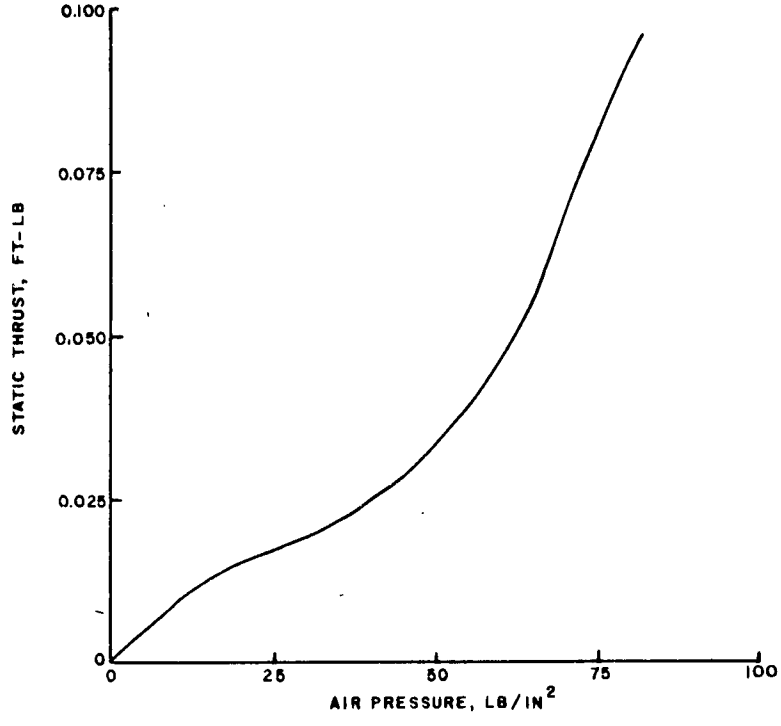

FIG. 9. Air Jet Static Thrust, F, Versus Air Pressure.

This section of the report has been devoted to the system devised to apply a turning torque to the telescope to reduce pointing errors. The system employs many nonlinear elements which are difficult to describe by conventional linear servomechanism analysis methods. It therefore seemed expedient to employ an analog computer on which nonlinear elements may easily be simulated.

The next section of this report is concerned with analog simulation of the complete tracking loop which includes the elements previously described, plus the sphere's moment of inertia and the damping provided by the thin film of water in the socket in which the sphere floats.

ANALOG COMPUTER INVESTIGATION

The use of a simple polar coordinate system for deriving the restoring torque as a function of the pointing error greatly simplifies the analysis of the system. At any instant, the restoring torque may be resolved into a plane defined by the torque vector and the axis of the telescope. Similarly, the moment of inertia of the sphere, and the viscous damping applied by the water film in the socket need only be considered about an axis perpendicular to the torque plane. A simple one-degree-of-freedom problem results as shown in Fig. 10.

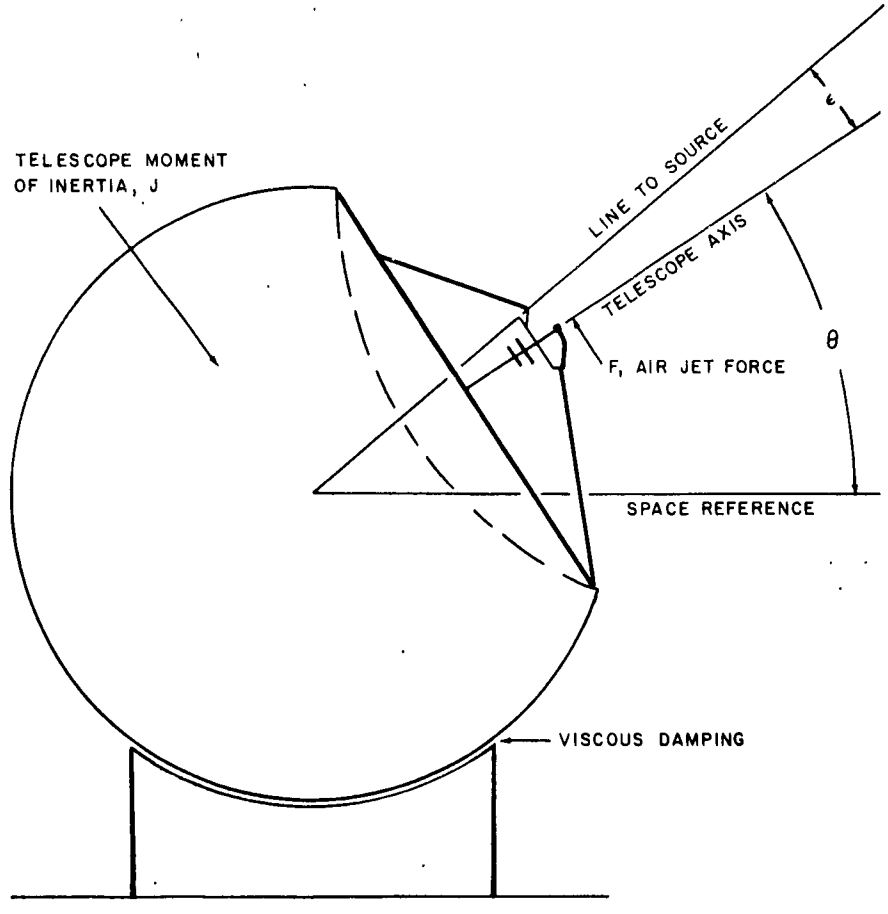

FIG. 10. Tracking Problem.

The equation describing the system is

$$J\ddot{\theta} + K_1\dot{\theta} + F\, f_T(\epsilon)\epsilon = 0 \quad , \tag{4}$$

where

θ = the angular position of the telescope in the plane of action with respect to inertial space

J = moment of inertia of the telescope about a diameter of the sphere perpendicular to the plane of action

K_1 = viscous damping coefficient in the plane of action

F = static torque of the air jet (1-foot moment arm)

$f_T(\epsilon)$ = torque attenuation factor

J, the moment of inertia of the telescope, is fixed and was found to be 0.11 slug-foot^2 in Appendix B.

K_1 was also computed in Appendix B and found to be 0.022 ft-lb/rad/sec.

Two of the parameters in the function $f_T(\epsilon)$ can be varied. The first of these parameters is the delay bias, V_2, which determines the dead zone and the shape of the γ versus $f_1(\epsilon)$ characteristic shown in Fig. 7. The second is the air pressure which governs the static thrust, F, of the air jet as described by Fig. 9.

Figure 11 is a system diagram of the analog computer used to simulate the performance of the tracking drive. The 3-cycle oscillator is adjusted to give an 8-volt peak sinusoidal output corresponding to 100% modulation of the 8-volt carrier amplitude across one half of the secondary of T_1 in Fig. 5. This signal is placed across potentiometer B in servo multiplier No. 1. The output taken from the arm of the potentiometer then corresponds to the scan modulation voltage appearing across one half of the secondary of T_1 in Fig. 5. The servo multiplier setting represents the modulation factor $f_1(\epsilon)$ shown in Fig. 7.

The output from the arm of potentiometer B is fed to a unity gain amplifier No. 31 where it is given a +8-volt offset corresponding to the average carrier level, V_3, in Fig. 6. Relay No. 1 acts as a voltage comparator which closes its contacts whenever V_3 falls below the voltage V_2-V_1 in Fig. 6. The closure of relay No. 1 represents the opening of the solenoid valve feeding the air jet.

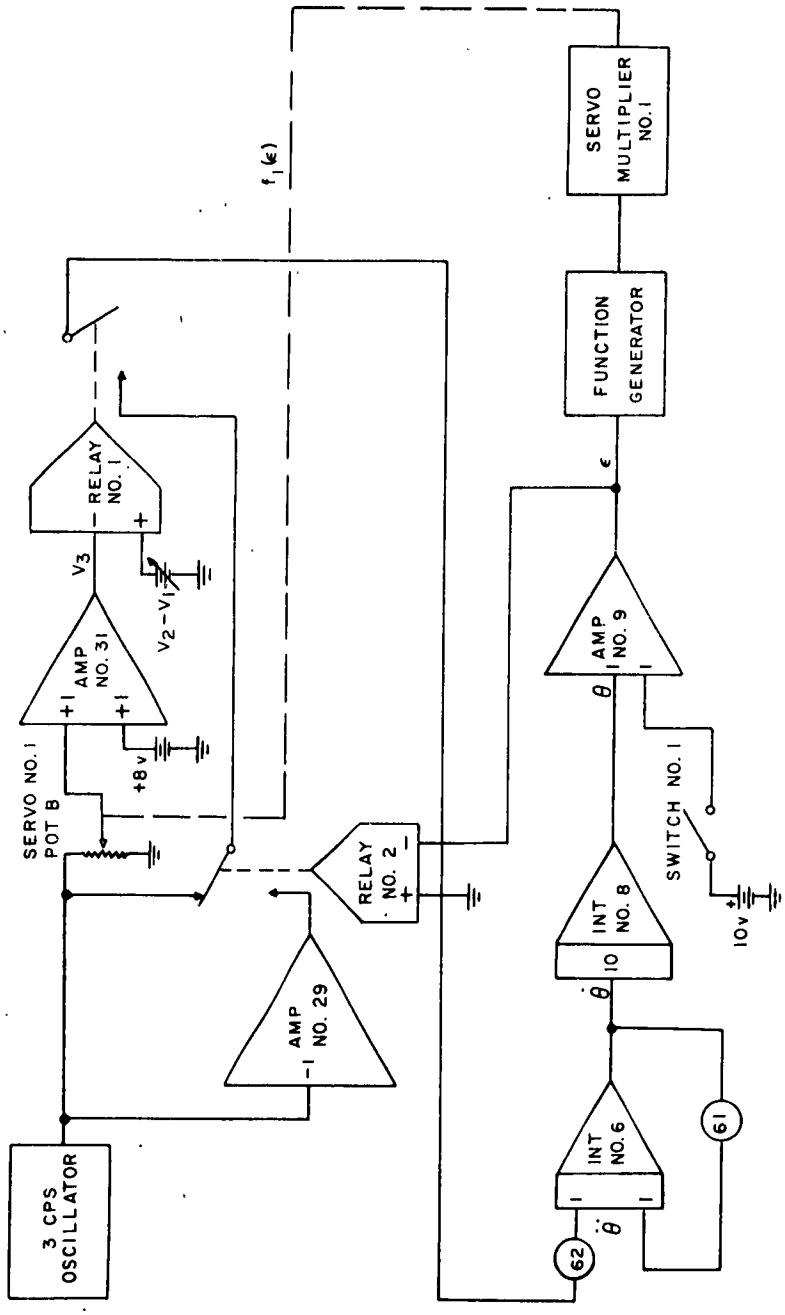

FIG. 11. Analog Computer System Diagram.

The variation of efficiency of the air jet with pulse width is easily computed. It was observed that the waveform at the output of the audio oscillator was the same as the component of useful torque available from the air jet at any instant in its rotation, i.e., the sine component of a rotating vector. The inverted output of unity gain amplifier No. 29 is selected by relay No. 2 whenever a negative torque is necessary. The output from relay No. 2 is fed through relay No. 1 and scale factor potentiometer No. 62. This signal then represents the restoring torque applied to the telescope by the tracking drive.

Equation 4 must now be rewritten, including the fixed constants of the telescope:

$$0.11\,\ddot{\theta} + 0.22\,\dot{\theta} + F\,f_T(\epsilon)\epsilon = 0$$

dividing by 0.11,

$$\ddot{\theta} + 0.2\,\dot{\theta} + \frac{F\,f_T(\epsilon)\epsilon}{0.11} = 0 \quad ,$$

and solving for $\ddot{\theta}$,

$$\ddot{\theta} = 0.2\,\dot{\theta} - 9.1\,F\,f_T(\epsilon)\epsilon \quad . \qquad (5)$$

Equation 5 must now be instrumented.

The input to the first unity gain integrator No. 6 will be assumed to be $\ddot{\theta}$. The first input to be considered is the correction torque, $9.1\,F\,f_T(\epsilon)$. Potentiometer No. 62 is set to a value so that $9.1\,F = 8 \times G_{62}$ where G_{62} is the gain through the potentiometer. The input to integrator No. 3 then has a scale factor of 1 volt per ft-lb. The output of integrator No. 6 is $\dot{\theta}$. $\dot{\theta}$ is fed back through potentiometer No. 61 to the input of integrator No. 6 to represent the viscous damping term $0.2\dot{\theta}$ of Eq. 5. The gain of potentiometer No. 61 is set so that $G_{61} = 0.2$.

The output of integrator No. 6 also drives integrator No. 8. The gain of integrator No. 8 was set to be 10; that is, a 1 volt-second input produces 10 volts output. The output of integrator No. 8, therefore, has the scale factor of 10 volts per degree. The output of integrator No. 8 is fed to unity gain amplifier No. 9, where it is summed with another input which represents a step input applied to test the response of the system. When switch No. 1 is closed, a 10-volt step is fed to amplifier No. 9. This step corresponds to a 1-degree step change in the angular position of the source.

The output of amplifier No. 9 then represents the error angle, ϵ, that is the difference between the axis of the telescope and the source direction line.

As ϵ reverses polarity, relay No. 2 changes the phase of the restoring torque as in the actual telescope drive. ϵ must now be shaped in order to approximate the $f_1(\epsilon)$ as plotted in Fig. 4. The characteristic of the function generator and succeeding servo multiplier which perform the operation are plotted as a dashed line in Fig. 4.

COMPUTER RESULTS

A number of analog computer runs were made in which the antenna position, θ, was plotted in response to a 1-degree step in target position as simulated by the closure of switch No. 1.

The first set of runs was made with K_1 = 0.022 ft-lb/rad/sec corresponding to the actual damping measured. F was set at 0.044 ft-lb, cooresponding to 60 psi/air pressure. V_2, the delay bias, was tried at three values: 7.6, 8.1, and 8.6 volts. The response of the system to a 1-degree step input is plotted in Fig. 12. At V_2 = 7.6 volts, it can be seen that the system is quite stable, but that a static pointing error, or dead zone, of approximately 0.1 degree is present. When V_2 is

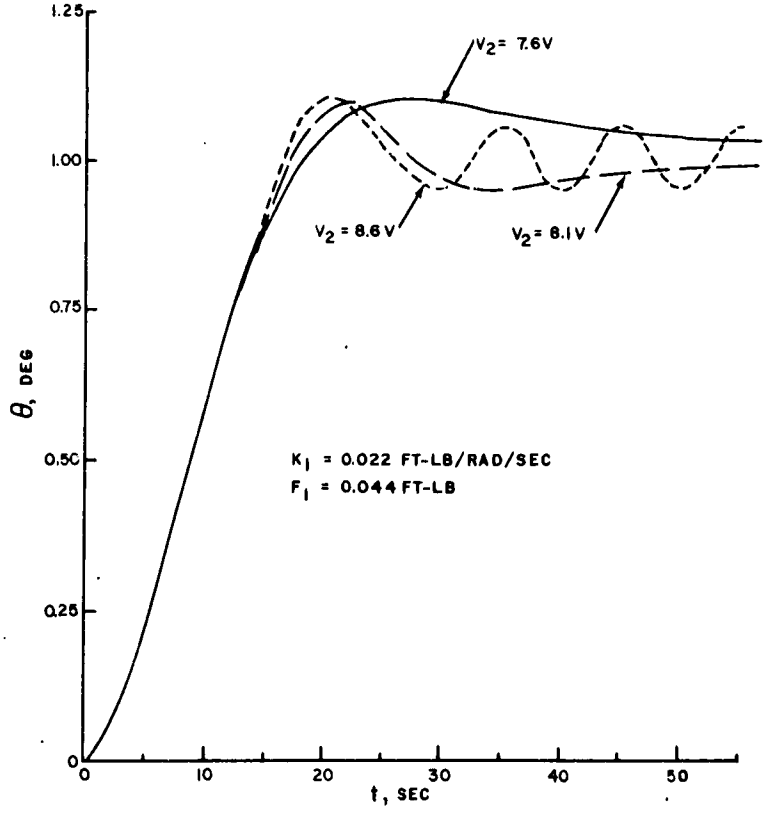

FIG. 12. Simulated System Response, Set No. 1.

set at 8.6 volts, the dead zone is zero and the system displays a small limit cycle oscillation in θ. This oscillation is due to the discontinuous nature of the γ versus $f_1(\epsilon)$ function for V_2 = 8.6 volts as shown in Fig. 7.

The second set of runs was made with K_1 changed to 0.066 ft-lb/rad/sec, or three times the actual value. The overshoots present in the first set of runs were eliminated, but the response time was greatly increased (see Fig. 13).

A third set of runs (Fig. 14) was made with K_1 remaining at 0.066 as before, but with F_1 increased to 0.088 ft-lb, corresponding to an air pressure of approximately 80 psi, the highest pressure at which the system was tested. The performance at V_2 = 7.6 and 8.1 volts was much improved over that of the first set of runs as far as stability was concerned. The response time has been decreased back to approximately the value of set No. 1 by the increase in air pressure.

A final run was made with the value of K_1 much higher than obtainable in the present model, in an attempt to attain greatly improved performance. The following values were used: K_1 = 0.066, F = 0.166, and V_2 = 8.4. The response of the system plotted in Fig. 15 reveals a very small dead zone, fast response, and excellent stability.

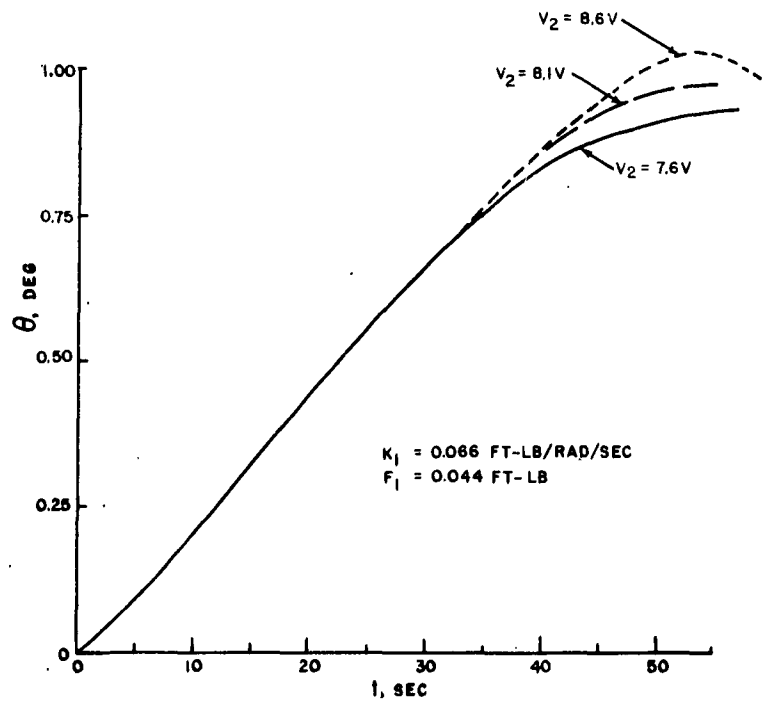

FIG. 13. Simulated System Response, Set No. 2.

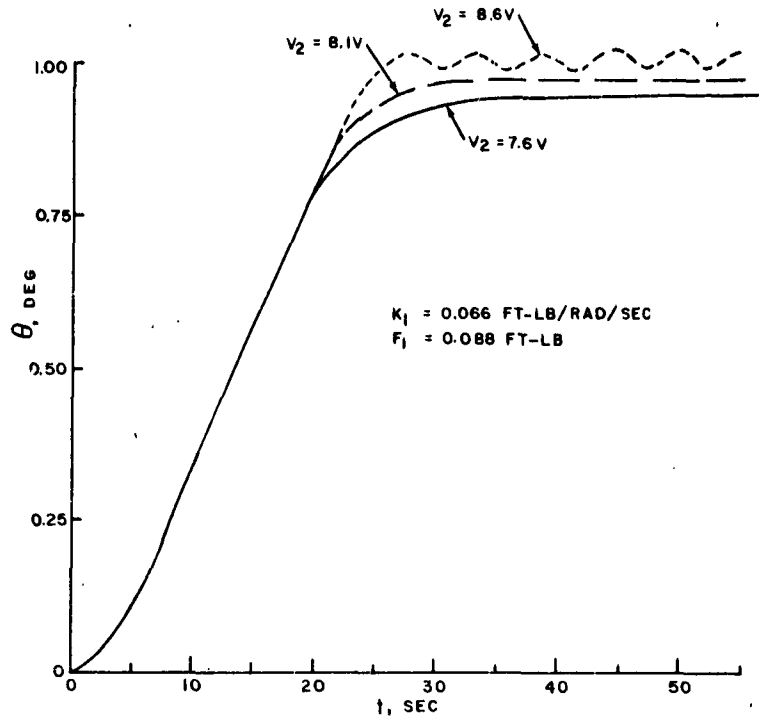

FIG. 14. Simulated System Response, Set No. 3.

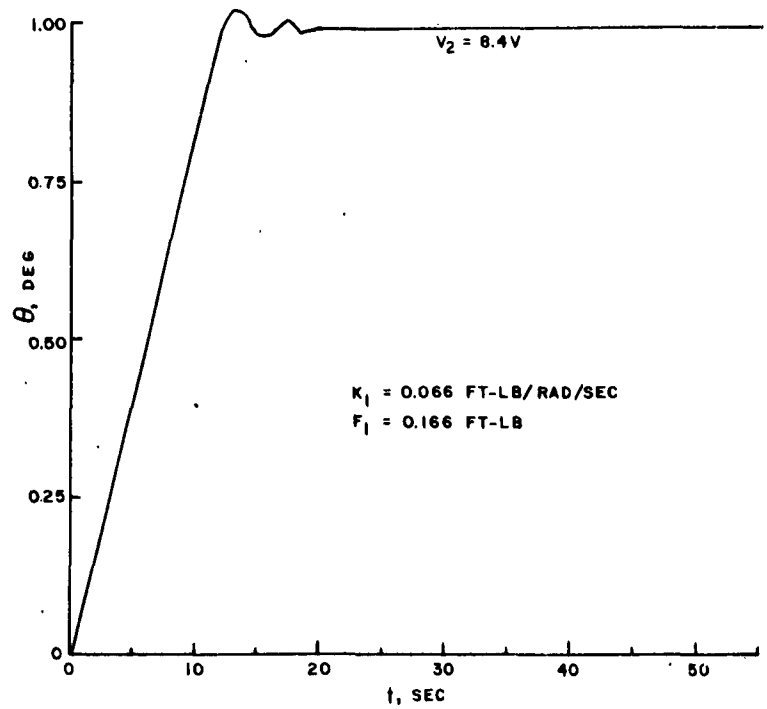

FIG. 15. Simulated System Response, Set No. 4.

EXPERIMENTAL RESULTS

Only the first of the five sets of analog runs discussed can be confirmed experimentally. The last four sets of data assume system parameters which were not possible with the present model. Lack of mechanical angular transducers in the sphere prevented actual readings of angular position versus time. Several meaningful criteria of system performance are easily observed, however. The response time, dead zone, and the number of overshoots in the response can be observed visually. These criteria are compared in Table 1 with the corresponding data derived from Fig. 12. The experimental results agree quite closely with the analog studies, confirming the validity of the computer studies.

TABLE 1. Actual and Simulated System Characteristics

Data source	V_2, volts	Response time, sec	Dead zone, deg	Number of overshoots
Computer	7.6	18.0	0.04	1
Model	7.6	16.0	0.06	1
Computer	8.1	17.5	0.02	2
Model	8.1	15.8	0.04	---
Computer	8.6	16.5	----	Oscillates
Model	6.6	15.0	----	Oscillates

K_1 = 0.022 ft-lb/rad/sec

F = 0.044 ft-lb

CONCLUSIONS

The analog simulation of the telescope drive has proved to be a very convenient and useful tool in predicting system performance. The total setup time on the computer was less than 6 hours; actual computer operating time was less than 30 minutes.

The computer indicated a problem in the model: the damping provided in the socket is insufficient for good system performance. To ensure stability, the gain and dead zone in the tracking torque had to be adjusted to the point where relatively poor system performance ensued.

A very simple method of augmenting the damping can be employed in future telescopes of larger size. A pair of gyroscopes can be attached to the movable portion of the telescope to sense angular rates about two mutually perpendicular axes both of which are in turn perpendicular to the axis of the parabola. The electrical outputs of the two gyroscopes can be converted from rectangular coordinates to the polar coordinates of the tracking drive. If the resulting polar coordinate rate signal is added electrically to $f_1(\epsilon)$, the pointing error signal, any amount of rate damping desired can be introduced. The small size of the present model would make it very difficult to add any gyroscopes at this time.

The greatly increased torque requirements of the angular drives for larger telescopes can be satisfied easily by use of a variable thrust rocket motor. Motors have already been constructed at NOTS that will easily fulfill the thrust and frequency response requirements of the drive.[5]

It is hoped that in the future a telescope can be constructed of the order of a 30-foot-diameter sphere. This unit will incorporate the improvements suggested and would be large enough to permit an insight into the problems of generating the spherical supporting surface and the parabolic surface. This unit would also reveal the seriousness of wind loads and thermal expansion problems which have not been quantitatively studied so far. If a 30-foot model operated in a realistic environment proved successful, it would point the way to a series of larger telescopes of similar design in the 100- or even the 1,000-foot diameter range.

---

[5]U. S. Naval Ordnance Test Station. The Design and Testing of a Variable-Thrust Rocket Motor (U), by Ronald F. Dettling. China Lake, Calif., NOTS, January 1962. (NAVWEPS Report 7803, NOTS TP 2799) CONFIDENTIAL.

Appendix A

FOCAL LENGTH OF A CENTRIFUGALLY CAST REFLECTOR

It has been found that the upper surface of a fluid confined in a cylindrical container assumes the shape of a parabola of revolution when the container is rotated at a constant speed about its axis.[6] It is necessary that the axis of rotation be vertical.

The focal length of the parabolic reflection can be expressed by the equation

$$FL = \frac{17,710}{N^2} \qquad (6)$$

where

FL = desired focal length in inches

N = the speed of rotation in revolutions per minute (rpm).

The use of epoxy resin as the fluid allows the retention of the parabolic surface. Surface finish of the paraboloid can be held to very close tolerances.

[6] Archibald, Paul B. "Epoxy Parabolic Mirrors," Modern Plastics, Vol. 34 (August 1957), pp. 116-117.

Appendix B

DETERMINATION OF THE MOMENT OF INERTIA AND DAMPING OF TELESCOPE

The moment of inertia, J, and damping factor, K_1, of the telescope model were determined as follows:

If the moving portion of the telescope is unbalanced by the removal of a known amount of lead shot ballast, the sphere will tend to rotate until the unbalance moment is zero, i.e., the heavy portion of the rotating system is directly down. The sphere is then manually rotated by an angle of 10 degrees from the vertical and then released. By observing the frequency and the damping of the oscillation, the moment of inertia and damping coefficient can be calculated. The equation of motion of the system can be written

$$J\ddot{\phi} + K_1 \dot{\phi} + rW \sin \phi = 0 \qquad (7)$$

where

J = moment of inertia of the sphere about a diameter, slug-ft^2

K_1 = viscous damping coefficient

r = radius of unbalance weight (W_1 = 1 foot)

W = unbalance weight (0.11 pound)

ϕ = the angle of rotation of the sphere from the equilibrium position.

By restricting ϕ to less than 10 degrees, the simplifying assumption that $\sin \phi = \phi$ can be applied to Eq. 7; that is,

$$J\ddot{\phi} + K_1 \dot{\phi} + rW\phi = 0 \quad ;$$

dividing by J,

$$\ddot{\phi} + \frac{K_1}{J} \dot{\phi} + \frac{rW}{J} \phi = 0 \quad . \qquad (8)$$

Equation 8 is of the form

$$\ddot{\phi} + 2\zeta \omega_n \dot{\phi} + \omega_n^2 \phi = 0 \quad , \tag{9}$$

in which

ζ = the damping ratio

ω_n = the undamped natural frequency .

By equating coefficients in Eq. 8 and 9,

$$\omega_n = \sqrt{\frac{rW}{J}} = \sqrt{\frac{0.11}{J}} \quad .$$

ω was observed to be approximately 1 rad/sec; therefore, J = 0.11 slug-foot^2. The solution for Eq. 8 is

$$\phi = \phi_{max} e^{-\zeta\omega_n t} \cos \omega_n \sqrt{1 - \zeta^2 t} \quad . \tag{10}$$

It is assumed that ζ is small, so that $\sqrt{1 - \zeta^2} = 1$. Equation 10 then becomes

$$\phi = \phi_{max} e^{-\zeta\omega_n t} \cos \omega_n t \quad . \tag{11}$$

The most convenient physical method of observing the damping factor is to measure the relative peak amplitudes of succeeding cycles.

The amplitude of ϕ at time t, can be written

$$\phi_1 = \phi_{max} e^{-\zeta\omega_n t_1} \cos \omega_n t_1$$

also

$$\phi_2 = \phi_{max} e^{-\zeta\omega_n t_2} \cos \omega_n t_2 \quad .$$

If

$$t_1 - t_2 = \frac{1}{\omega_n} \quad ,$$

$$\frac{\phi_1}{\phi_2} = \frac{\phi_{max}\, e^{-\zeta\omega_n t_1} \cos \omega_n t_1}{\phi_{max}\, e^{-\zeta\omega_n t_2} \cos \omega_n t_2} = \frac{e^{-\zeta\omega_n t_1}}{e^{-\zeta\omega_n t_2}} = e^{-\zeta\omega (t_1 - t_2)}$$

or

$$\frac{\phi_1}{\phi_2} = e^{-\zeta} \quad . \tag{12}$$

It was observed that the amplitude of the oscillation decreased by about 50% each cycle

$$e^{-\zeta} = 0.5 \qquad \zeta = 0.11 \quad .$$

The assumption that $\sqrt{1 - \zeta^2} = 1$ must be checked

$$\sqrt{1 - 0.1^2} = \sqrt{1 - 0.01} = \sqrt{0.99} = \text{approximately 1.}$$

From Eq. 7 and 8

$$K_1 = 2\zeta\, \omega_n J = 2(0.1)(1)(0.11) = 0.22 \text{ ft-lb/rad/sec.}$$

BIBLIOGRAPHY

Aseltine, John A. "Transform Method in Linear System Analysis," New York, McGraw-Hill, 1958.

Nixon, Floyd E. "Principles of Automatic Controls," New York, Prentice-Hall, 1953.

Savant, C. J. "Basic Feedback Control System Design," New York, McGraw-Hill, 1958.

NEGATIVE NUMBERS

FIG. 1, no negative number
FIG. 2, LO 75450
FIG. 3, LO 75449
FIG. 4 - 15, no negative numbers

INITIAL DISTRIBUTION

27 Chief, Bureau of Naval Weapons
- CD (1)
- CW (1)
- DLI-31 (2)
- R (1)
- R-2 (1)
- R-3 (1)
- RA (1)
- RA-2 (1)
- RA-3 (1)
- RAAV (1)
- RAAV-3 (2)
- RAAV-32 (2)
- RAAV-33 (1)
- RAAV-51 (1)
- RM (1)
- RM-3 (1)
- RM-371 (1)
- RM-373 (1)
- RMGA-4 (1)
- RMWC (1)
- RMWC-4 (1)
- RT (1)
- S (1)
- SEL (1)

2 Chief of Naval Operations
- OP-55 (1)
- OP-721D (1)

1 Chief of Naval Research (Code 104)
1 Naval Air Test Center, Patuxent River
1 Naval Avionics Facility, Indianapolis (Library)
2 Naval Missile Center, Point Mugu (Technical Library)
1 Naval Ordnance Laboratory, Corona
1 Naval Ordnance Laboratory, White Oak (Library)
1 Naval Postgraduate School, Monterey
2 Naval Research Laboratory
1 Naval Weapons Laboratory, Dahlgren (Technical Library)
2 Naval Weapons Services Office
1 Navy Electronics Laboratory, San Diego
1 Operational Test and Evaluation Force
1 Navy Liaison Officer, Tactical Air Command, Langley Air Force Base
1 Aberdeen Proving Ground (Ballistic Research Laboratories)
1 Army Electronic Proving Ground, Fort Huachuca (Technical Library)
1 Ordnance Test Activity, Yuma Test Station
1 Picatinny Arsenal (Library)
1 White Sands Missile Range (ORDBS-Technical Library)
1 Tactical Air Command, Langley Air Force Base (TPL-RQD-M)
1 Aeronautical Systems Division, Wright-Patterson Air Force Base (ASAPRD-Dist)
1 Air Force Cambridge Research Laboratories, Laurence G. Hanscom Field
1 Air Proving Ground Center, Eglin Air Force Base
1 Air University Library, Maxwell Air Force Base (AUL-6238)
10 Armed Services Technical Information Agency (TIPCR)
1 Defense Atomic Support Agency, Sandia Base
1 Ames Research Center
1 Langley Research Center (Library)
1 Armour Research Foundation, Chicago
2 Autonetics, A Division of North American Aviation, Inc., Downey, Calif.
- Dr. Robert Ashby (1)
- Technical Library, 393-53 (1)

ABSTRACT CARD

U. S. Naval Ordnance Test Station
An Angular Tracking Drive For a Radic Telescope of Unconventional Design, by John M. Boyle. China Lake, Calif., NOTS, December 1962. 30 pp. (NAVWEPS Report 8071, NOTS TP 3086), UNCLASSIFIED.

ABSTRACT. This report describes the reflector support and drive system for a large radio telescope of unconventional design. The telescope consists of a hollow sphere supported in a hydrostatic bearing formed by a concave socket filled with water. A

(Over)
1 card, 4 copies

U. S. Naval Ordnance Test Station
An Angular Tracking Drive For a Radio Telescope of Unconventional Design, by John M. Boyle. China Lake, Calif., NOTS, December 1962. 30 pp. (NAVWEPS Report 8071, NOTS TP 3086), UNCLASSIFIED.

ABSTRACT. This report describes the reflector support and drive system for a large radio telescope of unconventional design. The telescope consists of a hollow sphere supported in a hydrostatic bearing formed by a concave socket filled with water. A

(Over)
1 card, 4 copies

U. S. Naval Ordnance Test Station
An Angular Tracking Drive For a Radic Telescope of Unconventional Design, by John M. Boyle. China Lake, Calif., NOTS, December 1962. 30 pp. (NAVWEPS Report 8071, NOTS TP 3086), UNCLASSIFIED.

ABSTRACT. This report describes the reflector support and drive system for a large radio telescope of unconventional design. The telescope consists of a hollow sphere supported in a hydrostatic bearing formed by a concave socket filled with water. A

(Over)
1 card, 4 copies

U. S. Naval Ordnance Test Station
An Angular Tracking Drive For a Radio Telescope of Unconventional Design, by John M. Boyle. China Lake, Calif., NOTS, December 1962. 30 pp. (NAVWEPS Report 8071, NOTS TP 3086), UNCLASSIFIED.

ABSTRACT. This report describes the reflector support and drive system for a large radio telescope of unconventional design. The telescope consists of a hollow sphere supported in a hydrostatic bearing formed by a concave socket filled with water. A

(Over)
1 card, 4 copies

simple system of water pressure pads driven by a positive displacement pump keeps the sphere centered in the socket.

The drive system consists of a pulsed air jet or rocket motor that rotates about the axis of the telescope directly in front of the feed antenna. The drive system is unique in that it is independent of the orientation of the telescope with respect to the earth.

The theoretical and experimental portions of this report analyze the performance of the drive system of a two-foot-diameter model which automatically tracks an X-band source.

NAVWEPS Report 8071

simple system of water pressure pads driven by a positive displacement pump keeps the sphere centered in the socket.

The drive system consists of a pulsed air jet or rocket motor that rotates about the axis of the telescope directly in front of the feed antenna. The drive system is unique in that it is independent of the orientation of the telescope with respect to the earth.

The theoretical and experimental portions of this report analyze the performance of the drive system of a two-foot-diameter model which automatically tracks an X-band source.

NAVWEPS Report 8071

simple system of water pressure pads driven by a positive displacement pump keeps the sphere centered in the socket.

The drive system consists of a pulsed air jet or rocket motor that rotates about the axis of the telescope directly in front of the feed antenna. The drive system is unique in that it is independent of the orientation of the telescope with respect to the earth.

The theoretical and experimental portions of this report analyze the performance of the drive system of a two-foot-diameter model which automatically tracks an X-band source.

NAVWEPS Report 8071

simple system of water pressure pads driven by a positive displacement pump keeps the sphere centered in the socket.

The drive system consists of a pulsed air jet or rocket motor that rotates about the axis of the telescope directly in front of the feed antenna. The drive system is unique in that it is independent of the orientation of the telescope with respect to the earth.

The theoretical and experimental portions of this report analyze the performance of the drive system of a two-foot-diameter model which automatically tracks an X-band source.

1 Bell Telephone Laboratories, Inc., Murray Hill, N. J.
1 Burroughs Corporation, Detroit (Contract Manager)
1 Burroughs Corporation, Paoli, Pa. (Manager Technique Department)
1 Convair, San Diego (C. A. Wetherill)
1 Douglas Aircraft Company, Inc., Long Beach (Chief Engineer)
2 Douglas Aircraft Company, Inc., Santa Monica, Calif. (Testing Division Library)
2 General Dynamics, Pomona, Calif.
M. D. Phillips (1)
Engineering Librarian (1)
1 General Electric Company, Schenectady (LMEE Department, Librarian)
2 General Precision, Inc., Librascope Division, Glendale, Calif.
Engineering Librarian (1)
1 Grumman Aircraft Engineering Corporation, Bethpage, N. Y. (Library Director)
1 Hughes Aircraft Company, Culver City, Calif. (Research and Development Library)
1 Jet Propulsion Laboratory, CIT, Pasadena (Dr. W. H. Pickering)
1 Kearfott Company, Inc., West Paterson, N. J.
1 Litton Industries, Beverly Hills
1 Lockheed Aircraft Corporation, Burbank, Calif. (Electronics and Armament Systems Engineering, Kenneth W. Dickman)
1 Magnavox Corporation, Fort Wayne
1 McDonnell Aircraft Corporation, St. Louis (Engineering Library)
1 Minneapolis-Honeywell Regulator Company, Minneapolis (Librarian)
1 Norden Division, United Aircraft Corporation, Norwalk, Conn. (Library)
1 North American Aviation, Inc., Columbus, Ohio (Engineering Data Section)
1 North American Aviation, Inc., Space & Information Systems Division. Downey, Calif. (Technical Information Center, 4-096-314)
1 Northrop Corporation, Norair Division, Hawthorne, Calif.
1 Philco Corporation, Philadelphia, via InsMat
1 Republic Aviation Corporation, Farmingdale, N. Y. (Director of Military Contracts)
1 Specialties, Inc., Charlottesville, Va. (Dr. E. S. Gwathmey)
1 Stavid Engineering, Inc., Plainfield, N. J. (E. V. Wind)
1 Texas Instruments, Inc., Dallas
1 The Bendix Corporation, Bendix Pacific Division, North Hollywood (W. P. Boyer)
1 The Boeing Company, Seattle (G. S. Schairer)
1 The Boeing Company, Wichita
1 The Martin Company, Baltimore
1 The Rand Corporation, Santa Monica, Calif. (Aero-Astronautics Department)
1 Vought Aeronautics, Dallas
1 W. L. Maxson Corporation, New York (C. Schmidt)
1 Westinghouse Electric Corporation, Baltimore (Engineering Librarian)